15TH IEA HEAT PUMP CONFERENCE
MAY 26–29, 2026 | HOFBURG
VIENNA 2026
DECARBONISATION THROUGH INNOVATION

Study of Borefield Connection Configurations in Single-Pipe District Geothermal Heating and Cooling Systems Using a Simulation Test Bed

Rodney Hurt[a,*], Kevwe Ejenakevwe[a], Nurayn Tiamiyu[a], Gang Wang[b], Li Song[a]

[a]University of Oklahoma, 660 Parrington Oval, Norman, OK 73019
[b]University of Miami, 1320 S Dixie Hwy, Coral Gables, FL 33146

Abstract

Single pipe geothermal district heating and cooling networks (GDHCN) operate with ambient loop temperatures to provide service fluid to multiple buildings while using the soil as a heat source or heat sink. This work investigates single-pipe GDHCN configurations using a simulation test bed. The network connects three buildings with distinct load profiles: balanced, heating-dominant, and cooling-dominant. An appropriately sized bore field is designed for each building. Two sizing strategies were tested: individual sizing based on peak loads and integrated sizing using net system load. Performance metrics include annual electricity consumption and peak power demand of heat pumps under varying layouts, including even-spaced pairs (each bore field placed downstream of its building), partial clustering (two buildings grouped with their respective bore fields) and complete clustering (all three buildings grouped with their bore fields). Results show that the studied configuration changes have negligible impact on total system energy use, with annual consumption differences below 1%. However, building-level performance varies slightly due to upstream loads affecting entering fluid temperature and seasonal COP trends. Bore field sizing based on the system net load reduced total drilling depth by 42% without significant performance penalties, indicating potential for cost reduction. These findings suggest that while configuration alone does not substantially influence system-wide energy performance (up to 0.4% difference among different configurations), it may affect individual building efficiency (up to 1.5% difference) and become more critical in larger or less balanced networks. Future research should examine variable-speed pump control, expanded network topologies, and economic implications under diverse load conditions.

Keywords: Geothermal district heating and cooling; Geothermal network performance; Bore field clustering

1. Introduction

To mitigate climate change, the European Union aims to reduce CO_2 emissions by 55% by 2030 and achieve climate neutrality by 2050 [1]. The building sector plays a significant role in this transition, accounting for over one-third of global energy-related CO_2 emissions [2]. Within buildings, heating and cooling accounts for about 35% of total energy consumption [3], and a considerable fraction of this energy comes from fossil fuels. Thus, district heating and cooling networks (DHCN) have gained increasing attention as a promising approach to building decarbonization, especially due to their ability to exploit waste heat sources through a network of thermally interconnected buried pipes [4].

Presently, the focus is on DHCN operating with loop temperatures close to ambient conditions, thereby reducing thermal losses in the distribution pipes [5]. This has led to several transitions of DHCN from the 1st generation to the 5th generation (5G) of DHCN. Also, this shift towards low-temperature loops has necessitated

* *Corresponding author. Tel.: +1-405-325-1744*
E-mail address: Rodney.D.Hurt-1@ou.edu

the integration of geothermal energy into DHCN [6]. Thus, the focus of this paper is on 5th generation geothermal DHCN (GDHCN).

Reviews on the state-of-the-art of GDHCNs reveal a gap: while many studies optimize individual design choices, there is still limited understanding of how different design configurations – across subsurface design, hydraulics/control, and network topology/plant configuration – interact to determine overall techno-economic performance. These configurations can be grouped into (1) subsurface considerations (soil properties, bore field geometry and spacing, GHE (ground heat exchanger) type); (2) hydraulic considerations (control strategies, pump selection, pipe properties, etc); (3) network topology and plant configuration.

Several works have advanced understanding of subsurface and hydraulic layers, often in ways that implicitly condition the outcomes of network-level studies. For example, a review on shallow geothermal energy systems for heating and cooling [7] emphasizes that recent technological advancements focus on improved materials and innovative structures, alongside optimization of system-level parameters like pipe radius and spacing, dryness fraction, GHE length, number of GHEs, pump speed and flow rates, and soil thermal conductivity. This focus on parameter-level optimization is complemented by another review [6] which broadens the subsurface design by discussing foundation structures and buried civil infrastructure as novel GHEs. Building on this subsurface theme, Babak [8] investigated spiral GHEs using four models, demonstrating that GHE geometry can affect bore field performance. Relatedly, Tiamiyu et al. [9,10] compared four methods for sizing vertical GHEs – rule-of-thumb, two-pulse, ASHRAE, and GLHEPro-based reference – using data from a validated Modelica-based GSHP (ground-source heat pump) model simulated for both cooling- and heating-dominant climates. Using GHE inlet temperature and 20-year electrical energy consumption as metrics, they found the GLHEPro-based approach best maintained inlet temperature within heat pump operating limits while minimizing long-term energy consumption. Importantly, this implies that GHE sizing methodology is a vital design component that can propagate into network temperature trajectories, pumping needs, and long-term economics – and thus should be coupled more explicitly to topology and control studies.

In parallel, hydraulic and control research shows that operational strategy can dominate performance even when physical topology is fixed, reinforcing the need for integrated configuration analysis. Sommer et al. [5] proposed a single loop 5G GDHCN to address control challenges in commonly used double-loop DHCN. Using Modelica for both architectures and annual simulations, they found the single-loop design incurred less than a 2% increase in heat pump electricity consumption, while pumping electricity was highly sensitive to operating strategy: variable mass flow produced less than 1% increase, whereas constant mass flow rates caused a 48% increase. They also showed that double-loop network requires twice the pipe length of a single-loop configuration, highlighting an explicit capex-opex coupling between topology (pipe length) and hydraulics (pumping energy). However, they recommended further research for the single-loop DHCN such as investigating the impact of different demand profiles. Responding to this, Hurt et al. [11] evaluated a 5G single-loop GDHCN under different control strategies and load profiles using a validated Modelica model. The validation was done using baseline data from a community with a mix of residential buildings (serviced by air-source heat pumps) and commercial buildings (serviced by a bore field, a cooling tower and a boiler). The control strategies include constant pump speed operation and multiple variable speed modes. They reported that coordinated variable-speed control – maintaining a preset temperature difference across bore fields, keeping loop temperature within a desired range, and holding differential pressure in secondary loops – achieved a 47% reduction in overall energy consumption and a 54% reduction in carbon emissions relative to the baseline. Both [5] and [11] indicate that conclusions about best network architectures are inseparable from how the network is controlled, and that control can either erase or amplify the pumping penalties implied by the hydraulic design.

Contrarily, in network topology and configuration, only a limited number of studies exist and are not holistic – often because they simplify load diversity, ground-side dynamics or control. Huang et al. [12], developed a TRNSYS model of a solar assisted GSHP system and found that integrating domestic hot water (DHW) improves ground thermal balance, reduces hot water energy consumption by 70%, increases COP by 9.4%, and lowers annual operating cost by about 11% at modest added equipment cost. This is a critical bridge across layers: plant-side integration (DHW/solar) acts as a ground-thermal management mechanism, directly affecting the long-term bore field conditions that sizing studies such as [9,10] use as performance constraints. De Carli et al. [13], investigated optimal GDHCN designs in mild climates based on load density (low and medium) and district layout (single district versus two sub-districts with separate plants). They reported that GDHCN are more suitable in medium density areas and that sub-districting may reduce initial financial risk. However, because their district loads were residential and similar, the study could not examine the impact of load diversity – a factor that can be decisive as demonstrated in [14] where an exergy-based thermodynamic assessment of a bidirectional double-loop DHCN showed that higher load density improves exergy efficiency, and that sufficiently high load diversity can allow even low-density DHCNs to outperform aggregated individual building systems. This complements [13] by suggesting that density-driven conclusions may not generalize once diversity is introduced, and also complements [5,11] by implying that topology comparisons (single versus double) should be considered under diversity-driven operating conditions. Similarly, [15] proposed a toolchain (URBANopt + Modelica + EnergyPlus) to assess layout configurations for 5G DHCNs using life-cycle cost analysis, finding that under low-diversity conditions (three identical office buildings), a radial (unidirectional) topology is more economical than ringed or meshed grids. Read alongside [14], this result indicates that the choice of best topology may be conditional on diversity: radial may be optimal in low-diversity cases, but alternative topologies could become more attractive when diversity is high and bidirectional exchange benefits increase. However, the impact of high load diversity was not investigated in [15] to confirm this. Another tool was proposed in [16] to map the economic potential of 5GDHCN across US residential communities, using loads, building characteristics, and energy prices, with bore fields sized via GHEDesigner [17] supported by climate/ground lookup tables. While this enables large-scale screening of favorable locations, it does not optimize configurations for a given site.

The above reviews reveal that while existing studies have investigated various aspects of 5G GDHCN, not much attention has been given to studying the impact of factors like load diversity and load density in 5G single-loop GDHCN which according to [5], offers some more advantages than conventional bi-directional double-loop DHCN. Also, for the few network topology and configuration studies on GDHCN, it is unclear what sizing methods were used for the bore fields, which is critical for proper performance evaluation [9]. This suggests that probably, the bore field used in these studies were sized by the rule-of-thumb method which is mainly based on the largest peak load between cooling and heating load [18]. But to conduct a more holistic investigation on the impact of the above factors such as load diversity and load density, it is necessary to use a suitable sizing method such as the GLHEPro method which was demonstrated to be more accurate in [9] as the calculation procedure is more rigorous than other methods. Therefore, this study investigates the impact of load diversity and load density on the performance of a single loop 5G GDHCN, sized with the GLHEPro method.

2. Methodology

The methodology outlines the modelling approach and design assumptions used to evaluate the performance of a single-pipe geothermal district heating and cooling network. It describes the system components, sizing procedures, and simulation framework applied to analyse the impact of load diversity, load density, and bore field configuration on energy performance. The following subsections detail the building load profiles, heat pump modelling, bore field design, and network configuration tested in this study.

2.1. Building Load Model

The geothermal network was constructed with three buildings and three bore fields. Each building has a unique load profile for space cooling and space heating, as shown in Fig. 1. Building (a) has a balanced load profile, Building (b) is heating dominant, and Building (c) is cooling dominant. Each building was modelled with multiple zones so space heating and cooling may be required simultaneously.

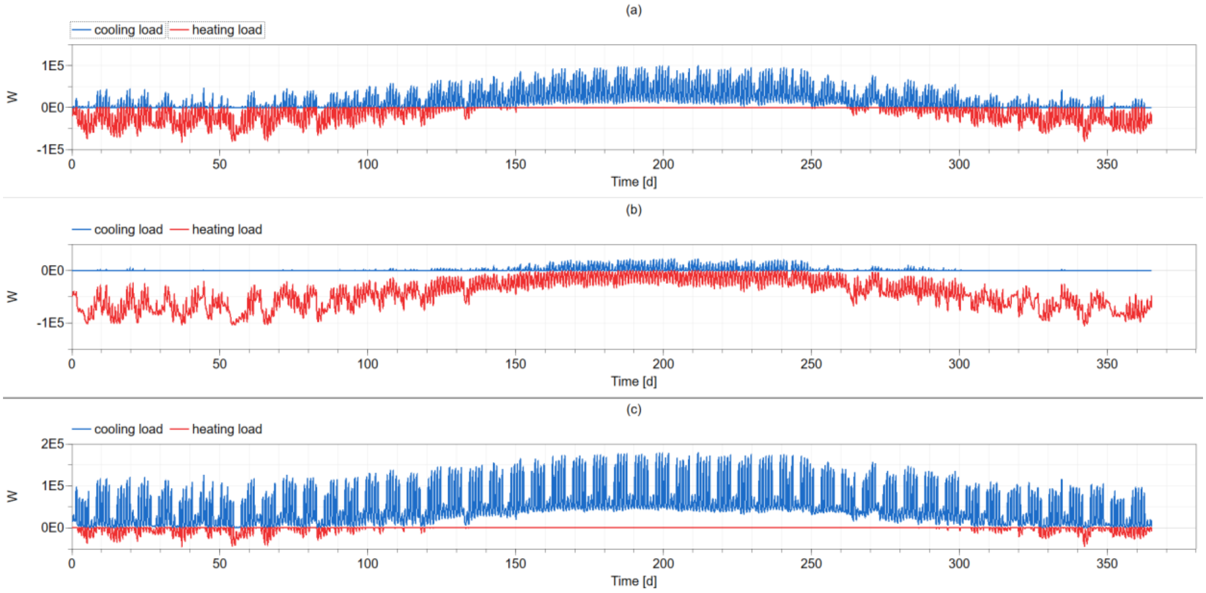

Figure 1: Building Load Profiles (a) Balanced (b) Heating Dominant (c) Cooling Dominant

Design conditions of each building load profile are summarized in Table 2. Water flow rate is based on the peak design load for each building. It is designed as a constant volume system.

Table 1: Building Load Information

Building Load Profile	Peak Heating Load (W)	Peak Cooling Load (W)	Water Flow Rate (kg/s)
Balanced	189093	227605	0.84
Heating Dominant	243072	51415	0.90
Cooling Dominant	101357	412269	1.53

2.2. Heat Pump Model

The heat pumps are modelled using a performance curve that is a regression of the coefficient of performance (COP) taken from manufacturer data [19]. Factors affecting the COP include indoor air conditions, entering fluid temperature, and operating mode (heating or cooling). The system is modelled as constant volume so mass flow rate will not affect the COP. The COP calculation is shown in Eq. (1) where T_f is the temperature of fluid entering the heat pump, T_{air} is either the dry bulb or wet bulb indoor air temperature, and $a_0 - a_5$ are regressed coefficients. This relationship results in both the power consumption and net heat transfer into the heat carrier fluid due to each building load.

$$COP = a_0 + a_1 T_f + a_2 T_f^2 + a_3 T_{air} + a_4 T_{air}^2 + a_5 T_f T_{air} \quad (1)$$

Each building was modeled with one heat exchanger for all cooling load and one for all heating load. This was necessary because each building has simultaneous heating and cooling at some time steps. It is assumed that the space heating and space cooling loads are exactly matched by the heat pumps at each timestep. This introduces slight error to the model as a physical system would have some variation in zone air conditions, notably in systems with binary or staged operation. However, the effects of this error are reduced when modelled over a significant time span. The mass flow rate of water through the heat pump is constant so it does not appear in the COP calculation.

Since the building loads are assumed to be perfectly matched, the indoor air temperatures will be constant. Therefore, the COP calculations can be simplified to the following in Eq. (2) and Eq. (3) when the indoor dry bulb temperature is 18.4°C for heating and the wet bulb temperature is 18.4°C for cooling. The resulting COP curves over standard fluid operating temperatures are shown in Fig. 2. Both operating modes have similar COP values around 28°C but suffer in extended fluid temperature ranges.

$$COP_{heat} = -68.67 + 0.4504 T_f - (6.8 * 10^{-4}) T_f^2 \quad (2)$$

$$COP_{cool} = 8.4060 - 0.0603T_f + (1.10 * 10^{-4})T_f^2 \tag{3}$$

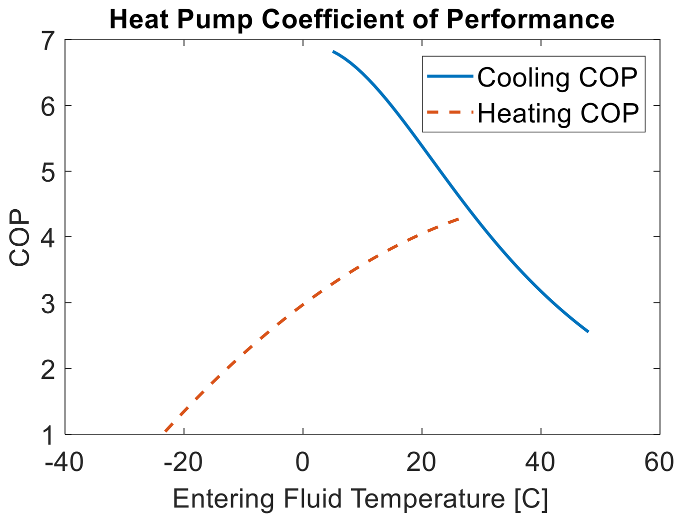

Figure 2: Heat Pump COP with Respect to Fluid Temperature

Heat transferred to the fluid as a result of the building loads is given in Eq. (4) and Eq. (5), where q_{heat} represents heat pumps in heating mode and q_{cool} represents those in cooling mode. $q_{b,h}$ and $q_{b,c}$ are the building heating and cooling loads, respectively. P_{heat} and P_{cool} represent the power consumed by the heat pump in heating mode and the heat pump in cooling mode.

$$q_{heat} = q_{b,h} - P_{heat} = q_{b,h}\left(1 - \frac{1}{COP_{heat}}\right) \tag{4}$$

$$q_{cool} = q_{b,c} + P_{cool} = q_{b,c}\left(1 + \frac{1}{COP_{cool}}\right) \tag{5}$$

Power required by an individual heat pump is given in Eq. (6). P is the power demand of an individual heat pump in heating or cooling mode. q_b and COP are the respective building load and COP of the same heat pump.

$$P = \frac{q_b}{COP} \tag{6}$$

2.3. Bore Field Model

This study utilized the bore field model developed by Lawrence Berkely National Lab as part of the Buildings Library [20]. This model allows for a wide range of customizations based on the use case. U-tube bores with varying geometries and layouts are used in this study.

Each bore field has been sized based on the corresponding building load profile. For example, the bore field that accompanies the heating dominant building has different mass flow rate and building load profile than that of the balanced load profile. The bore fields were sized in two ways using GLHEPro. First, a bore field for each building load profile was designed independently of the others as if there would be three separate systems. There is no consideration for any heat that may be transferred between buildings to reduce the net load.

The design method is an iterative process in which a single bore is designed to account for the entire building load using the finite line source model. The total length is then separated into equal lengths for a bore field grid. The grid layout is initially determined by best judgement and iterated upon to meet constraints such as desired well depth, or available space. The input parameters for the bore field design are given in Table 2. These are based on material properties of commonly installed systems. External properties, such as soil thermal conductivity or far field temperature, are based on conditions local to Oklahoma, USA or estimates from literature.

Table 2:Bore Field Design Input Parameters

Property	Value	Note
Thermal conductivity of pipe (W/m.K)	0.4	High Density Polyethylene
Inner radius of the pipe (m)	0.0127	
Thickness of the pipe (m)	0.0037	
Shank spacing (m)	0.0462	Spacing from center of bore to center of pipe
Thermal conductivity of soil (W/m.K)	1	
Specific heat capacities of soil (kJ/Kg.K)	0.95	
Volumetric heat capacities of soil (kJ/Km3)	1.9	
Average annual ground temperature (°C)	16.9	
Thermal conductivity of grout material (W/m.K)	0.8	Bentonite Grout
Specific heat capacity of grout material (kJ/Kg.K)	2.5	
Volumetric heat capacities of grout material (kJ/Km3)	4.5	
Design heat pump minimum inlet temperature (°C)	6	
Design heat pump maximum inlet temperature (°C)	38	

The final design parameters of each bore field are given in Table 3. The larger peak loads of the heating dominant and cooling dominant buildings require larger bore fields.

Table 3: Full Bore Field Design Parameters

Property	Balanced Load	Heating Dominant	Cooling Dominant
Borehole Configuration (number of borehole)	2 ×3 (6)	3 × 4 (12)	3 ×4 (12)
Total Borehole depth (m)	637	1367	1581
Field Borehole Depth (m)	106	114	132

The next bore field design took heat transfer between buildings into consideration. The net heating load and net cooling load of all buildings was used to determine the total length of a single well for the entire system. This value was then used to scale each bore field from the original size. The reduced bore field sizes are given in Table 4. This design reduced the total drilled depth by 42% from 3585m to 2081m.

Table 4: Reduced Bore Field Design Parameters

Property	Net Load Design	Balanced Load	Heating Dominant	Cooling Dominant
Borehole Configuration (number of borehole)	4 × 4 (16)	2 ×2 (4)	2 ×3 (6)	2 ×3 (6)
Total Borehole depth (m)	2081	370	794	918
Field Borehole Depth (m)	130	92	132	153

2.4. Geothermal Network Configuration

The geothermal network is a single pipe distribution system with three buildings, three bore fields, and a circulating pump. Connections to each building allow for bypass flow as they have different design flow rates. Each building is equipped with a distribution pump operating at a constant speed. Bore fields do not have any bypass flow.

Three system configurations were made in which bore field connection points were changed. Buildings followed the same order in each configuration. The balanced load profile is directly after the circulation pump, followed by the heating dominant building and then the cooling dominant building. The three configurations were then repeated after replacing the bore fields with the reduced size versions.

The order of bore field connections follow that of the building load profile: balanced, heating dominant, and cooling dominant. Configuration 1 (even-spaced pairs) in Fig. 3 has a low load density in which case the buildings are evenly spaced around the primary loop with their corresponding bore field located downstream of each building. Configuration 2 (partially clustering) in Fig. 4 first has a medium load density with the heating dominant and cooling dominant buildings clustered together, followed by their respective bore fields. While the balanced building and its bore field are upstream to the cluster. Configuration 3 (completely clustering) in Fig. 5 has a high load density where all three buildings are clustered together and the three bore fields are clustered together downstream of the farthest building.

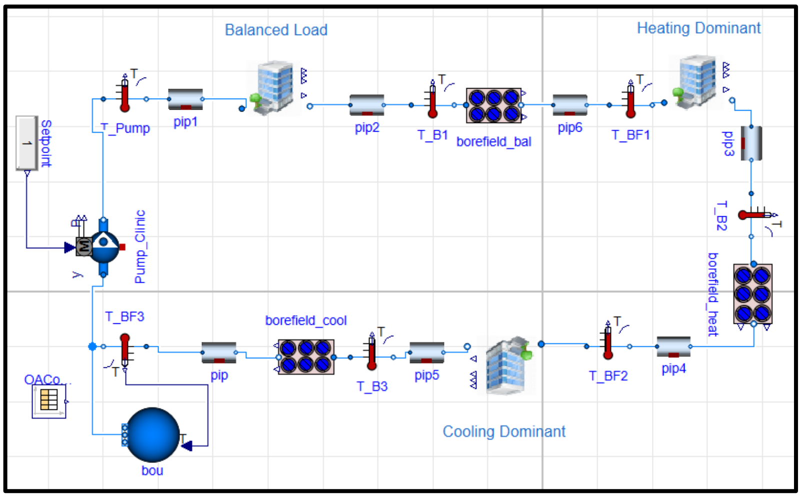

Figure 3: Geothermal Network - Configuration 1

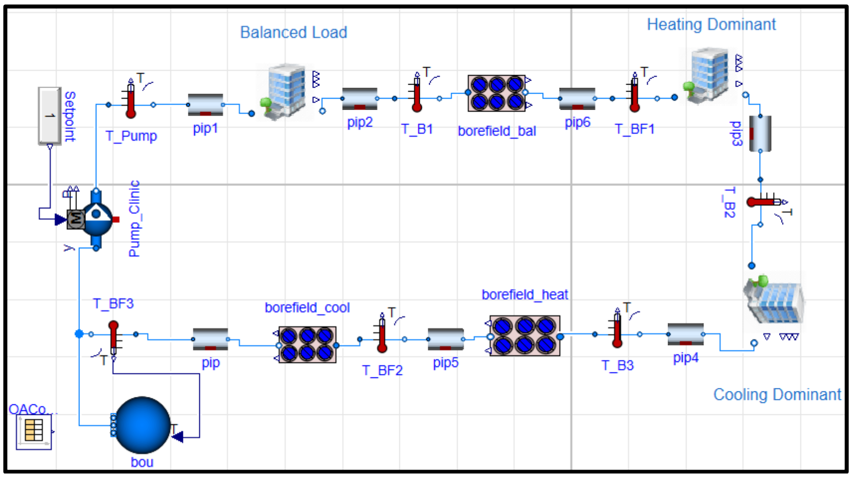

Figure 4: Geothermal Network - Configuration 2

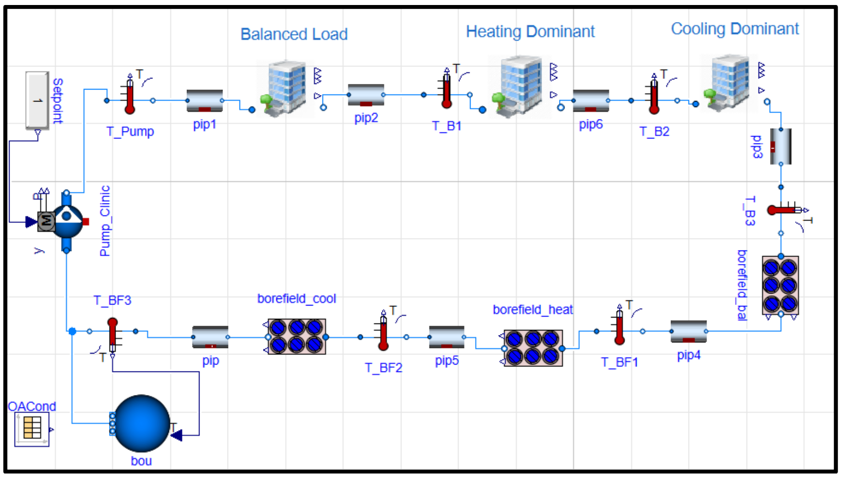

Figure 5: Geothermal Network - Configuration 3

In practice, the clustered bore fields in configurations 2 and 3 may be designed as a single larger bore field. However, this configuration offers a better comparison as the flow will be in series between bore fields rather than parallel. Additionally, a single bore field would result in different thermal interference between individual wells. The method tested does not introduce additional interference.

3. Results and Discussion

The primary performance metrics under consideration are the peak power demand and the annual electricity consumption of heat pumps in each configuration. In Configuration 1, heat is rejected or absorbed from the bore field after each building. Configurations 2 and 3 have greater opportunity for certain buildings to directly impact the entering fluid temperature of downstream buildings. Larger inlet temperature variation will result in COP variation between heat pumps in separate buildings.

Figure 6 displays the power and cumulative energy consumption of all heat pumps in the system for each configuration. Both the power demand and cumulative electricity consumption are nearly equal for each configuration. Hydronic pump power was not included as it is constant and identical for all configurations.

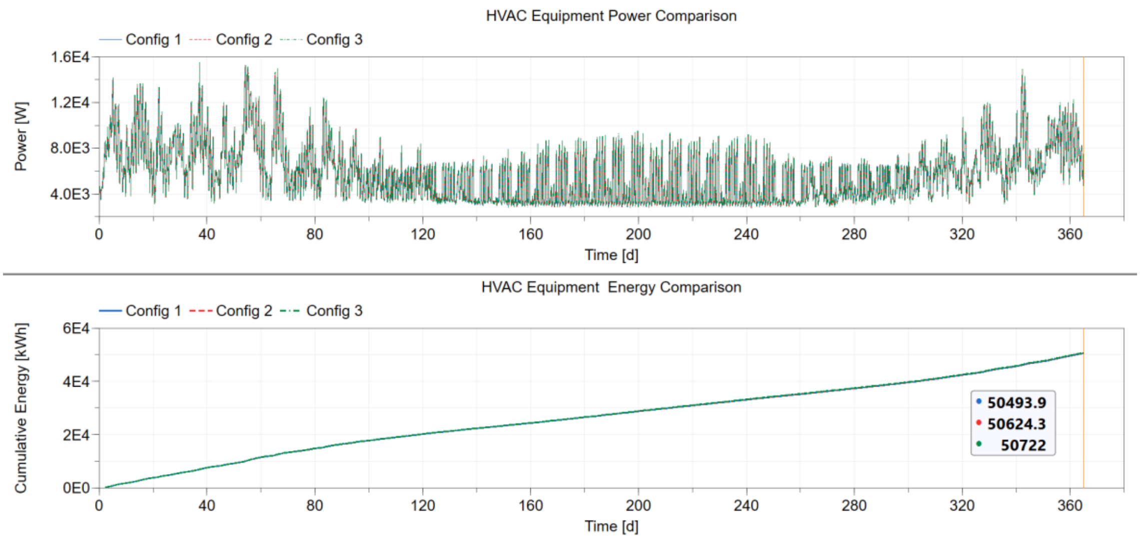

Figure 6: HVAC Power and Energy Consumption with Full Size Bore Fields

The power demand and electricity consumption are similar between configurations; however, there is some variation in both. Table 5 includes the peak power demand and the annual electricity consumption of all heat pumps in each configuration. Peak power demand occurred on day 37 for each configuration. Configuration 3 resulted in the largest power demand and consumption. This outcome is reasonable as upstream buildings have more effect on downstream buildings before heat can be transferred to the bore field.

Table 5: HVAC Power and Energy Consumption with Full Size Bore Fields

	Peak Power Demand [W]	Annual Electricity Consumption [kWh]
Configuration 1	14166.1	50296.0
Configuration 2	14268.5	50411.8
Configuration 3	14428.7	50520.4

The HVAC energy demand is impacted by the heat pump COP as the building loads are identical between configurations. Due to the fact that hydronic pump speeds and indoor air conditions are assumed to be constant, the COP will only be affected by the entering fluid temperature at each heat pump. The fluid temperature entering the balanced load profile building for each configuration is shown in Figure 7. There was a maximum temperature difference of 2.7°C, which occurred between Configuration 1 and Configuration 3. Figure 7 is only representative of one building. The cooling dominant and heating dominant buildings will have unique entering fluid temperatures.

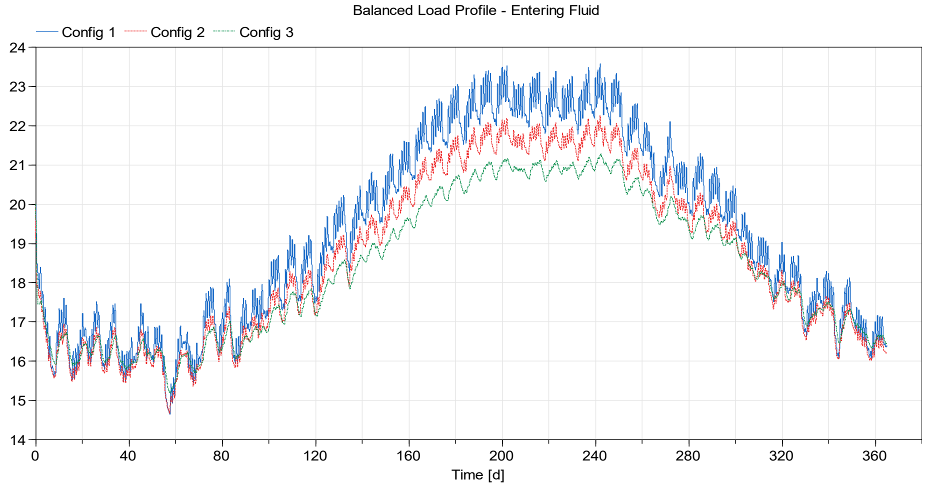

Figure 7: Balanced Load Profile Fluid Inlet Temperature

The COP curves of the balanced load profile building can be observed in Figure 8. As expected, the cooling COP of configuration 1 is the lowest because it has the highest entering fluid temperature. The COP has the largest variance between configurations during cooling season. This is likely because the entering fluid temperature is closer to the average soil temperature during heating season.

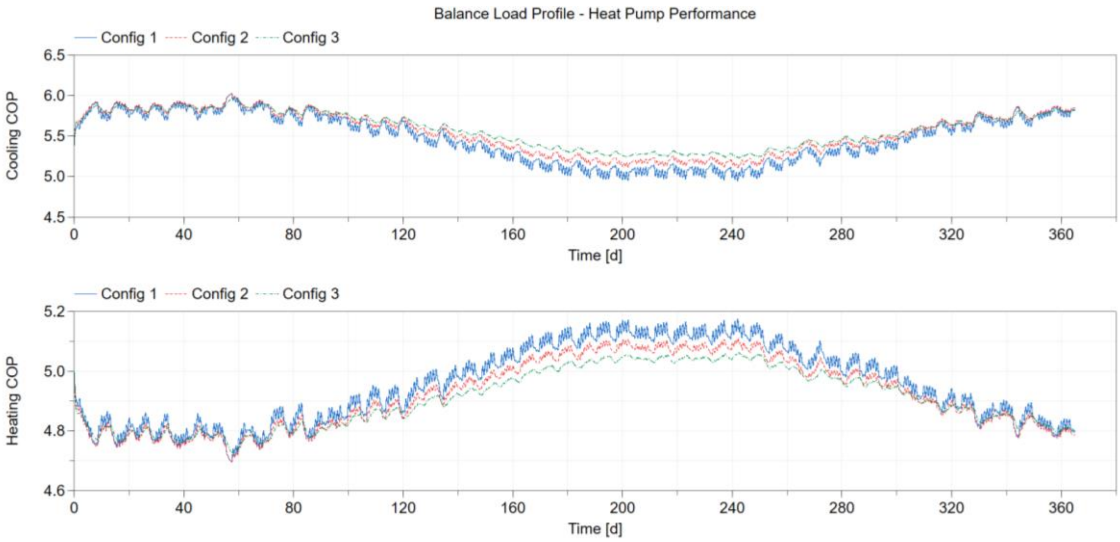

Figure 8: Heat Pump COP in Balanced Load Building

Configuration 3 has the highest cooling COP but the lowest heating COP on average. Configuration 1 is the inverse with the lowest cooling COP but the highest heating COP. Configuration 3 has a cooling COP 6.3% higher than Configuration 1 at the maximum, but a heating COP 2.4% lower. These observations only hold for the balanced load building in this system.

The COP curves of the heating dominant building are given in Figure 9 and of the cooling dominant building in Figure 10. Each building has a configuration with the best performing heating heat pumps and a different configuration with the best performing cooling heat pumps. Additionally, the highest performing cooling configuration results in the lowest performing heating in a given building for all cases.

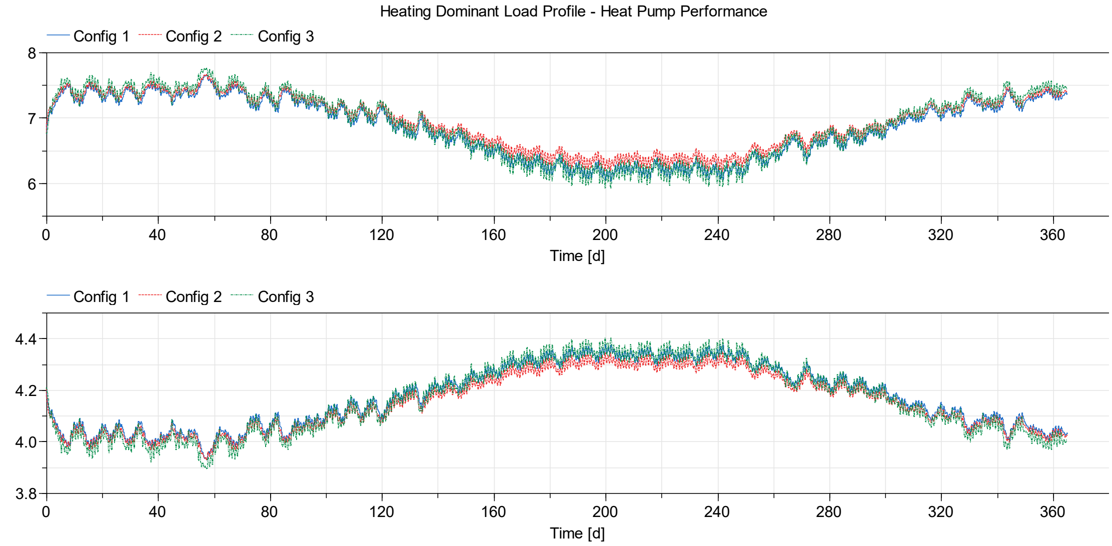

Figure 9: Heat Pump COP in Heating Dominant Building

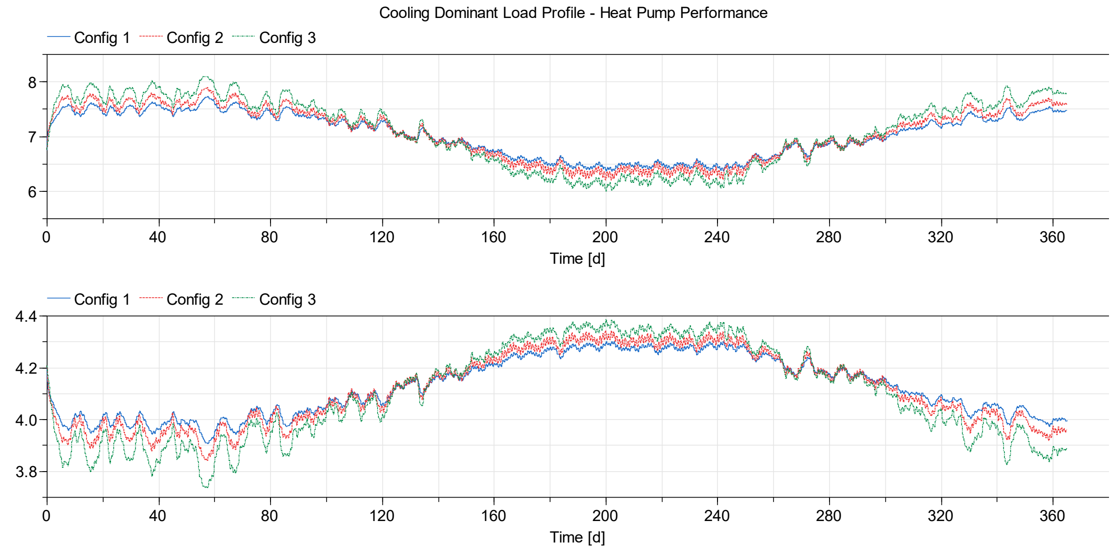

Figure 10: Heat Pump COP in Cooling Dominant Building

The performance of each configuration were studied with reduced bore field sizes. Reduced bore field sizes result in lower heat transfer capability to the soil and greater entering fluid temperature variation. This, in turn, affects the COP of each heat pump in the system. The same trends are followed with specific configurations resulting in the same best performance results. The total system performance with reduced bore field sizes can be seen in Fig. 10. The power demand and total consumption are nearly identical between configurations. However, both are greater than in the full size bore field configurations.

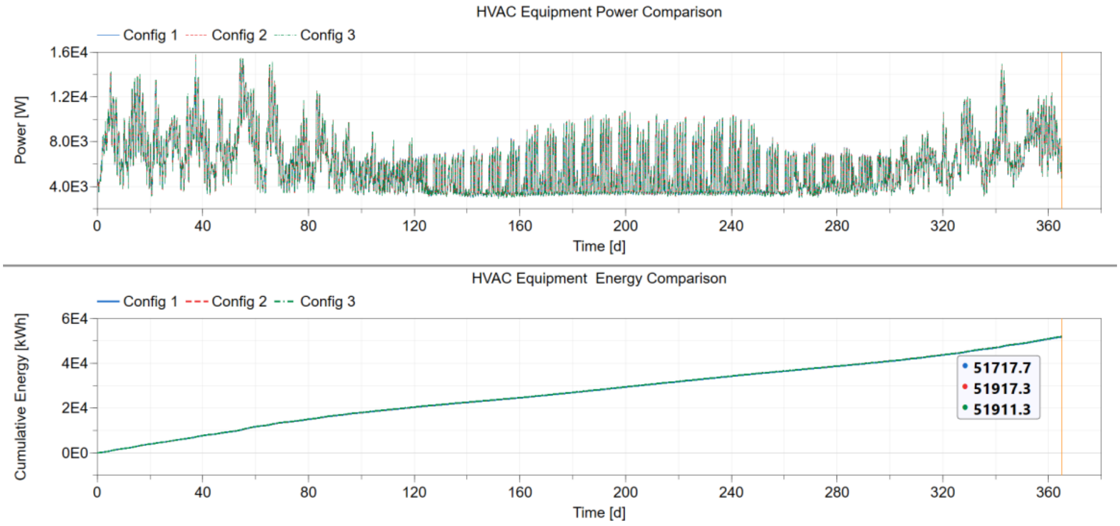

Figure 11: HVAC Power and Energy Consumption with Reduced Size Bore Fields

There are no substantial differences in power demand or annual consumption of the entire system between any configuration with like bore field sizes. However, Specific configurations may slightly benefit one or more building(s) depending on the load profiles. The annual HVAC electricity consumption for individual buildings in each configuration are given in Table 6 in which slight differences are present. Configuration 1 has the lowest total consumption but the highest consumption of the balanced load building.

Table 6: Annual Electricity Consumption of Individual Buildings

	Balanced Load [kWh] / Percent change from Configuration 1	Heating Dominant [kWh] / Percent change from Configuration 1	Cooling Dominant [kWh] / Percent change from Configuration 1	Total [kWh] / Percent change from Configuration 1
Original Bore Fields				
Configuration 1	11448 / NA	24699 / NA	14149 / NA	50296 / NA
Configuration 2	11374 / -0.65%	24833 / 0.54%	14205 / 0.4%	50412 / 0.23%
Configuration 3	11299 / -1.3%	24880 / 0.73%	14342 / 1.36%	50520 / 0.45%
Reduced Bore Fields				
Configuration 1	11935 / NA	24523 / NA	14874 / NA	51332 / NA
Configuration 2	11775 / -1.34%	24726 / 0.83%	15018 / 0.97%	51519 / 0.36%
Configuration 3	11603 / -2.78%	24794 / 1.11%	15108 / 1.57%	51505 / 0.34%

4. Conclusion

This study evaluated multiple configurations of a single-pipe geothermal district heating and cooling network to determine the impact of bore field placement and network layout on system performance. Results indicate that configuration changes have minimal influence on overall system performance, as annual electricity consumption and peak power demand remain nearly identical across all tested layouts (up to 0.4% 0.3%). Individual building performance does vary slightly (up to 1.5%), with certain configurations favoring heating or cooling efficiency depending on load profiles.

These findings are based on a network with a diverse and relatively balanced net load profile, where complementary heating and cooling demands offset most seasonal variations. Systems in this study included an accompanying bore field for each building. In scenarios with larger loads, shifted peaks, or unbalanced profiles, configuration effects may become more pronounced. Similarly, smaller bore fields, increased bypass flow, or expanded networks with more buildings and bore fields could introduce additional complexity and performance differences.

Future research can explore larger and more diverse networks with varying load densities and diversity. This includes scenarios with unbalanced net loads and with highly variable load profiles. Load profiles in the studied systems were relatively complementary in reducing the net load of all buildings. The effects of unique configurations may be more pronounced with non-complementary building loads. The economic implications for billing among individual buildings can also be considered as performance may be affected by upstream buildings. Lastly, it will be important to study systems with variable speed pump control. This may influence fluid temperature and heat pump performance.

Overall, network configuration alone does not significantly affect total energy consumption in the studied cases. It can influence building-level performance and may have greater impact under different design or operational conditions.

Nomenclature

COP	Heat pump coefficient of performance in either heating mode or cooling mode
T_{air}	Temperature of conditioned space, either dry bulb or wet bulb
T_f	Temperature of fluid entering heat pump
q_{heat}	Total heat absorbed from fluid by heating mode heat pump
q_{cool}	Total heat rejected to fluid by cooling mode heat pump
$q_{b,h}$	Heating load of building
$q_{b,c}$	Cooling load of building
P	Power demand of heat pump

References

[1] Delivering the European Green Deal - European Commission 2021. https://commission.europa.eu/topics/climate-action/delivering-european-green-deal_en (accessed November 10, 2025).

[2] Buildings - Energy System. IEA n.d. https://www.iea.org/energy-system/buildings (accessed November 10, 2025).

[3] Heating, Ventilation, Air Conditioning, Refrigeration, and Water Heating. EnergyGov n.d. https://www.energy.gov/eere/buildings/heating-ventilation-air-conditioning-refrigeration-and-water-heating (accessed November 10, 2025).

[4] Werner S. International review of district heating and cooling. Energy 2017;137:617–31. https://doi.org/10.1016/j.energy.2017.04.045.

[5] Sommer T, Sulzer M, Wetter M, Sotnikov A, Mennel S, Stettler C. The reservoir network: A new network topology for district heating and cooling. Energy 2020;199:117418. https://doi.org/10.1016/j.energy.2020.117418.

[6] Figueira JS, García Gil A, Vieira A, Michopoulos AK, Boon DP, Loveridge F, et al. Shallow geothermal energy systems for district heating and cooling networks: Review and technological progression through case studies. Renew Energy 2024;236:121436. https://doi.org/10.1016/j.renene.2024.121436.

[7] Ahmed AA, Assadi M, Kalantar A, Sliwa T, Sapińska-Śliwa A. A Critical Review on the Use of Shallow Geothermal Energy Systems for Heating and Cooling Purposes. Energies 2022;15:4281. https://doi.org/10.3390/en15124281.

[8] Dehghan B. B. Effectiveness of using spiral ground heat exchangers in ground source heat pump system of a building for district heating/cooling purposes: Comparison among different configurations. Appl Therm Eng 2018;130:1489–506. https://doi.org/10.1016/j.applthermaleng.2017.11.124.

[9] Tiamiyu N, Ejenakevwe KA, Song L. Performance Analysis of Vertical Borehole Ground Heat Exchanger Design Methods Using Modelica-Based Modeling and Simulation. 2024 ASHRAE Annu. Conf., ASHRAE; 2024. https://doi.org/10.63044/s24tia51.

[10] Tiamiyu N, Ejenakevwe KA, Hlanze P, Song L. Evaluating the performance of ground source heat pumps under different vertical borehole ground heat exchanger design methods using Modelica-based dynamic modeling and simulation. Sci Technol Built Environ 2025:1–18. https://doi.org/10.1080/23744731.2025.2583886.

[11] Hurt R, Ejenakevwe KA, Beaty J, Hlanze P, Wang G, Cai J, et al. A Simulation Study of Single Pipe Geothermal District Heating and Cooling Network Pumping Control Strategies and Performance. 2025 ASHRAE Annu. Conf., ASHRAE; 2025. https://doi.org/10.63044/s25asi19.

[12] Huang J, Fan J, Furbo S. Demonstration and optimization of a solar district heating system with ground source heat pumps. Sol Energy 2020;202:171–89. https://doi.org/10.1016/j.solener.2020.03.097.

[13] De Carli M, Galgaro A, Pasqualetto M, Zarrella A. Energetic and economic aspects of a heating and cooling district in a mild climate based on closed loop ground source heat pump. Appl Therm Eng 2014;71:895–904. https://doi.org/10.1016/j.applthermaleng.2014.01.064.

[14] Zarin Pass R, Wetter M, Piette MA. A thermodynamic analysis of a novel bidirectional district heating and cooling network. Energy 2018;144:20–30. https://doi.org/10.1016/j.energy.2017.11.122.

[15] Von Rhein J, Henze GP, Long N, Fu Y. Development of a topology analysis tool for fifth-generation district heating and cooling networks. Energy Convers Manag 2019;196:705–16. https://doi.org/10.1016/j.enconman.2019.05.066.

[16] Simpson JG, Beckers KF, Allard DA, Chen Y, Das P, Ho J, et al. National Modeling of Geothermal District Energy Systems with Ambient-Temperature Loops Using dGeo: Preprint. Renew Energy 2024.

[17] West TN, Spitler JD. Ground heat exchanger design tool with RowWise placement of boreholes. Sci Technol Built Environ 2024;30:1148–66. https://doi.org/10.1080/23744731.2024.2386882.

[18] Ahmadfard M, Bernier M. A review of vertical ground heat exchanger sizing tools including an inter-model comparison. Renew Sustain Energy Rev 2019;110:247–65. https://doi.org/10.1016/j.rser.2019.04.045.

[19] WaterFurnace International. Versatec 500 0.75-6 Ton Installation Manual. 2024.

[20] Picard D, Helsen L. Advanced Hybrid Model for Borefield Heat Exchanger Performance Evaluation, an Implementation in Modelica, 2014, p. 857–66. https://doi.org/10.3384/ecp14096857.